Title

Ecogenomic sensor reveals controls on N2-fixing microorganisms in the North Pacific Ocean

Journal

The ISME Journal: Multidisciplinary Journal of Microbial Ecology, 8(6)

ISSN

1751-7362

Authors

Robidart, Julie C
Church, Matthew J
Ryan, John P
et al.

Publication Date

2014-06-01

DOI

10.1038/ismej.2013.244

Peer reviewed

Ecogenomic sensor reveals controls on N_2-fixing microorganisms in the North Pacific Ocean

Authors: Julie C. Robidart[1,2,3]*, Matthew J. Church[3,4], John P. Ryan[2], François Ascani[3,4], Samuel T. Wilson[3,4], Deniz Bombar[1,3], Roman Marin III[2], Kelvin J. Richards[3,4], David M. Karl[3,4], Christopher A. Scholin[2,3], Jonathan P. Zehr[1,3]

Affiliations:

[1]Department of Ocean Sciences, University of California Santa Cruz, 1156 High Street, Santa Cruz, CA 95064 USA.

[2]Monterey Bay Aquarium Research Institute, 7700 Sandholdt Road, Moss Landing, CA 95039 USA.

[3]Center for Microbial Oceanography: Research and Education, University of Hawaii, 1950 East-West Road, Honolulu, Hawaii 96822 USA.

[4]Department of Oceanography, University of Hawaii, 1000 Pope Rd., Honolulu, HI 96822 USA.

*Corresponding author: Department of Ocean Sciences, University of California Santa Cruz, 1156 High Street, Santa Cruz, CA 95064 USA; 831-459-3560; jrobidart@ucsc.edu

Running Title: Ecogenomic sensing of marine nitrogen-fixers

Subject Category: Microbial population and community ecology

Abstract

Nitrogen-fixing microorganisms (diazotrophs) are keystone species that reduce atmospheric dinitrogen (N_2) gas to fixed nitrogen, thereby accounting for much of N-based new production annually in the oligotrophic North Pacific. However, current approaches to study N_2 fixation provide relatively limited spatiotemporal sampling resolution, hence little is known about the ecological controls on these microorganisms or the scales over which they change. In the present study, we utilized a drifting robotic gene sensor to obtain high-resolution data on the distributions and abundances of N_2-fixing populations over small spatiotemporal scales. The resulting measurements demonstrate that concentrations of N_2 fixers can be highly variable, changing in abundance by nearly three orders of magnitude in less than 2 days and 30 kilometers. Concurrent shipboard measurements as well as long-term time-series sampling uncovered a striking and previously unrecognized correlation between phosphate, which is undergoing long-term change in the region, and N_2-fixing cyanobacterial abundances. These results underscore the value of high-resolution sampling and its applications for modeling the effects of global change.

keywords: autonomous sensing / biosensors / diazotrophs / microbial oceanography / nitrogen fixation / time-series

Introduction

Dinitrogen (N_2)-fixing microorganisms are important sources of new nitrogen (N) in N-limited ocean regions worldwide (Carpenter and Capone, 2008) and are responsible for sustaining a large fraction of carbon export from surface waters to depth in major ocean basins (Karl et al 2012). Molecular tools to quantify these organisms have become available in recent years, however, such tools typically rely on traditional oceanographic ship-based sampling and their application is thus limited. New developments using *in situ* chemical sensing and continuous time-series export sampling in the oligotrophic open ocean have demonstrated the importance of episodic events in modulating marine biogeochemical cycles (Johnson et al 2010; Karl et al 2012; Ascani et al., 2013), but the variety of processes we can sample and sense continuously at the microbial level *in situ* is extremely limited. As a result it has been difficult to determine how ephemeral environmental fluctuations control the growth and activities of N_2-fixing microbes and how such fluctuations might be used to gain a perspective of how longer-term trends such as global environmental change will impact these keystone species.

The development of "ecogenomic sensors" (Preston et al 2011) has in part been driven by this challenge of enabling autonomous, high-resolution quantification of microbial nucleic acids *in situ*. In this study we deployed one of these devices, the Environmental Sample Processor (ESP; Figure 1D; Scholin, 2013), with coupled physical and biogeochemical sensors on a drifter near the long-term biogeochemical time-series Station ALOHA in the North Pacific Subtropical Gyre (NPSG). Our objective was to determine the scales at which N_2- fixing microorganisms change and the environmental controls on their abundances. The resulting datasets reveal links that are important to

predicting the abundances of N_2-fixing microorganisms with respect to long-term changes in nitrogen and phosphorus concentrations, such as those that have been documented at Station ALOHA (Karl et al 2001).

Materials and Methods:

ESP preparation.

During an oceanographic research cruise aboard the R/V Kilo Moana from September 6 – 21, 2011 (KM 11-25, BioLINCS: Biosensing Lagrangian Instrumentation and Nitrogen Cycling Systems) intensive sampling for microbial abundances and activities was conducted within the NPSG using autonomous instrumentation and shipboard sampling. The ESP was deployed on a drifting platform as described previously (Ottesen et al 2013) with an Acoustic Doppler Current Profiler (ADCP) and conductivity-temperature-depth sensor (CTD) mounted to the ESP base. The ESP was fitted with quantitative PCR (qPCR) reagents for detecting *nifH* genes from *Trichodesmium, Atelocyanobacterium,* and *Crocosphaera* and qPCR reaction conditions and kinetics were validated in the laboratory prior to deployment (as in Preston et al 2011; Robidart et al 2012; Supplementary Table 1). The ESP was maintained in an air-conditioned room until deployment, and qPCR standard curves were verified upon recovery of the instrument to check reagent stability and instrument calibration. The assay for *Crocosphaera* failed this post-recovery standard curve check and is not included in analyses presented here. Changes in the bacterioplankton community composition were also measured on the ESP using ribosomal RNA (rRNA) probes in a sandwich hybridization array format to detect Bacterial and Archaeal clades from a bulk sample lysate as described previously (Preston et al 2009; Table 1). Spot intensity of

each hybridization probe (an average of 8 spotted probes per target) were background-subtracted and changes in the picoplankton community were calculated based on relative sample-to-sample variation in spot intensity for each target over time.

Shipboard Sample Collection.

Aboard the ship, discrete seawater samples were collected from CTD rosette bottles fired at 5, 25, 45, 75, 100, 125, 150, 175 and 200 m near the ESP over the course of the cruise. Flow cytometric analyses and all biogeochemical measurements were performed according to the Hawaii Ocean Time-series (HOT) sample analytical protocols found at http://hahana.soest.hawaii.edu/hot/methods/results.html . For nucleic acid analyses, 2 L samples were collected from 25 ± 0.5 m at 12 stations (Supplementary Figure 1), filtered onto 0.22 um Supor filters with a 10 um pore size prefilter and immediately frozen in liquid nitrogen. Samples were shipped to the lab at UCSC and stored at -80ºC until processing.

Community Analyses. DNA extractions were carried out in the lab as described (Moisander et al 2010) with a Qiacube (Qiagen) to carry out the column-based extraction portion of the protocol according to the manufacturer's instructions.

Lab-based qPCR was carried out using Taqman Gene Expression Master Mix (Applied Biosystems) and with optimized assay conditions as in Supplementary Table 1. *Synechococcus phnD* gene assays were developed and optimizations were performed with Accuprime qPCR mix (Invitrogen) with an added 2.5mM $MgCl_2$ per 30µl reaction. Cross-reactivity tests were performed between each *Synechococcus* cluster (Clade II clusters 1 & 2, and Clade III) and all assays were specific to their targets at concentrations above 10 copies per reaction (Supplementary Figure 7). Non-target clade

concentrations were not high enough to change gene quantifications over this time series, for any of the assays. *phnD* is present as one copy per genome in sequenced genomes from different clades of *Synechococcus*, and here we assume this is the same for *Synechococcus* in the environment (Ilikchyan et al., 2010).

Biogeochemical Analyses.

BioLINCS CTD rosette sampling collected samples from nine discrete depths in the upper ocean: 5, 25, 45, 75, 100, 125, 150, 175 and 200 m. For subsequent analyses of inorganic nutrients, 125 - 500 ml seawater was subsampled from the CTD rosette bottles into 125 or 500 ml acid-washed polyethylene bottles and frozen upright until nutrient analyses. On shore, high-sensitivity nutrient measurements were conducted from photic zone waters according to (Karl and Tien 1992; Dore and Karl 1996). Nutrients from the deeper samples were analyzed using a 6-channel Bran & Luebbe Autoanalyzer III as described in "HOT Laboratory Protocols" (http://hahana.soest.hawaii.edu).

Remote sensing.

Eddies and advective anomalies were described using sea level anomaly data from AVISO (Archiving, Validation and Interpretation of Satellite Oceanographic data), combined microwave and infrared SST data from Remote Sensing Systems and surface chlorophyll data from MODIS (Moderate Resolution Imaging Spectroradiometer) Aqua (Figure 1). The life history of Eddy A (trajectory and size of the eddy) was analyzed with a searching algorithm using a Gaussian SLA profile. Size is defined as the width of the Gaussian and depicted by the size of the red circles in Supplementary Figure 3. SLA for the Station ALOHA region for Supplementary Figure 4 were gathered and assembled

from the Colorado Center for Astrodynamics Research (http://eddy.colorado.edu/ccar/ssh/hist_global_grid_viewer).

HOT data were obtained from the Hawaii Ocean Time-series Data Organization & Graphical System (HOT-DOGS: http://hahana.soest.hawaii.edu/hot/hot-dogs/). Near-monthly *nifH* gene abundances measured at Station ALOHA from 2008 – 2011 were quantified according to (Church et al 2005; Church et al 2008). In this study, we define "summer" as any time at which temperatures at 25m depth exceeded 25.6ºC (corresponding with ca. July 1 to Nov 15), and for comparability, we define "spring" as an equal number of days prior to "summer." These dates roughly correspond with the official dates of each season but we chose to place quantitative restraints on the dates in order to compensate for inter-annual differences.

Results

High-resolution Lagrangian sampling.

The drifting ESP sampled every 16 hours over a 10-day period (September 7-16, 2011) approximately 160 km north of Station ALOHA (Figure 1A). In this region, eddy-forced advection is evident as the anticyclonic wrapping of relatively warm, chlorophyll-enriched water around eddy A (Figure 1A). The warm filament along the northern periphery of eddy A is the most pronounced signature of this advection, indicating eastward flow in that area. A westward counter-flow between eddy A and eddy B is suggested by the westward deflection of SST isotherms in that region, corresponding with the westward transport of the ESP. Lateral mixing between the eddy-stirred water

160 types is indicated by the patchiness evident in the higher-resolution and more synoptic
161 SST (Figure 1B), and by water column salinity along the drift track (Figure 1C).
162 The ESP quantified N_2-fixing microorganism ("diazotroph") nitrogenase (*nifH*)
163 gene abundances by qPCR assays. The instrumented autonomous platform (ESP, ADCP
164 and CTD) sampled within the upper mixed layer at 24 m depth, drifting northeastward for
165 6 days before turning west for the final transit (Figure 1). The ESP drift track relative to
166 satellite altimetry indicates that the instrument sampled within the eddy periphery while
167 traveling northeastward (Eddy A, Figure 1A). Salinity and temperature averaged 35.19 ±
168 0.09 and 26.09 ± 0.20 °C, respectively, during this drift period (Figure 2).
169 The abundances of diazotrophs (as inferred from qPCR *nifH* gene quantifications)
170 differed between the various genera of N_2-fixing bacteria, including the unicellular
171 cyanobacterium genus *Atelocyanobacterium* (Thompson et al 2012), the filamentous
172 cyanobacterium *Trichodesmium* and an uncultivated *nifH*-gene-containing group of
173 proteobacteria (Church et al 2005). *Trichodesmium* abundances were extremely patchy,
174 with a 140-fold increase during one period of 32 hours and 30 km during the first portion
175 of the *in situ* experiment and a 218-fold decrease during a 32 hour and 29 km observation
176 period near the end of the instrument drift (Figure 3B). The maximum *Trichodesmium*
177 *nifH* abundances in our study are among the highest reported near Station ALOHA since
178 2005 (Fong et al 2008; Figure 3A). Surprisingly, the unicellular *Atelocyanobacterium*
179 were also abundant, and despite the quasi-Lagrangian nature of drifter sampling, even
180 more variable than *Trichodesmium* abundances, fluctuating by nearly three orders of
181 magnitude in *nifH* copies (from 4.3×10^2 to 2.4×10^5) per liter over one 32 hour, 22 km drift
182 period (Figure 3B).

Shipboard Verification of ESP qPCR Abundances.

ESP-measured diazotrophs abundances were confirmed by samples collected using the ship's CTD rosette system (Figure 2D), which was deployed < 6 km from the ESP (with most samples taken < 1 km from the ESP; Supplementary Figure 1). The patterns of *Trichodesmium* abundances determined from shipboard sampling were generally similar to those observed by the ESP, with high variability in abundances occurring over the first three days of the deployment. Although shipboard *Trichodesmium* abundance measurements were the same order of magnitude as the abundances reported by the ESP, they were less variable, with a 32-fold (n=9) change in density over the sampling period relative to 218-fold change observed using the ESP (n=14; Table 1). This discrepancy is likely due to the heterogeneous distributions of *Trichodesmium* and the higher frequency of ESP sampling. The extraordinary patchiness in these samples is illustrated by an 8-fold change in *Trichodesmium* concentration over a single 7 km, 13 hour span. The patterns of *Atelocyanobacterium* densities as determined by shipboard sampling were also similar to those obtained by the ESP overall, with high variability, ranging from 2.1×10^2 to 5.3×10^4 *nifH* copies per liter over a single 26 km, 24 hour period (Figure 2D).

The ESP rRNA abundance patterns for several dominant, non-N_2-fixing microbial groups including *Prochlorococcus*, *Synechococcus* and picoplanktonic heterotrophs (Preston et al 2009), were used to evaluate heterogeneity in the broader population. In contrast to the diazotrophs, the concentrations of these prokaryotes were relatively constant, varying less than 2.5-fold over the entire deployment (Table 1). Flow cytometric quantifications of *Prochlorococcus*, *Synechococcus*, picoeukaryotes and

206 heterotrophs supported the population stability observed using the ESP probe arrays
207 (Table 1). The maximum variation by ship-based flow cytometry was in the
208 *Synechococcus* population which varies by a factor of only 1.92. In stark contrast,
209 patchiness in diazotroph populations far exceeded that of these other groups of microbes,
210 with the lowest degree of variation in the *Trichodesmium* population, with a 32-fold
211 degree of variation in *nifH* qPCR abundance (Table 1). For all diazotrophs, this
212 measured population heterogeneity (maximum ÷ minimum abundace) was at least 16
213 times higher than that of other measured microbial populations.

214 In order to determine whether this high heterogeneity was specific to N_2 fixing
215 microorganisms or more generally represented fluctuations in phylogenetically-
216 constrained groups (the *nifH* targets specific, low-abundance genera while more broadly-
217 characterized taxa are identified by flow cytometry and rRNA hybridization probes), we
218 also quantified *phnD* gene abundances of three clades of *Synechococcus* that have similar
219 abundances to the diazotrophs (on the order of 10^5 cells per L at 25m depth). These
220 clades varied by a maximum of 20-fold (less than 10% and 3% of the observed variability
221 in *Trichodesmium* and *Atelocyanobacterium*, respectively) during the 10 day sampling
222 period (Table 1). Diazotroph populations were more heterogeneous than populations of
223 clades of cyanobacteria with similar abundances.

224 We compared our data to several years of summertime N_2-fixing cyanobacteria
225 abundances measured at Station ALOHA (Figure 3). While populations did not decrease
226 to below detection limits during the BioLINCS cruise, observed changes in abundances
227 during this quasi-Lagrangian time-series were comparable to the range of changes in

summertime abundance detected over all measured (3-6 total) summers at station ALOHA for two of the three nitrogen-fixing cyanobacteria (Figure 3).

Relationships between diazotroph abundances and ocean biogeochemistry.

Abundances of N_2-fixing microbes correlated strongly with salinity (*Atelocyanobacterium* Pearson R value = -0.91, $P<0.05$, n=14), despite high population heterogeneity. The significant, negative correlation between salinity and phosphate (Pearson correlation R = .99, $P<0.05$, n = 8) translates to a significant positive correlation between *Atelocyanobacterium* abundances and calculated phosphate concentrations (using ESP-coupled CTD salinity: [PO4] = ((-.371 * salinity) + 13.09) along the western edge of Eddy A (R = 0.91, $P<0.05$; n=14, Figure 4, S2). The ADCP mounted on the ESP revealed that the drifting instrument was largely moving with the currents, in terms of direction and speed, during this phase of the transit (Figure 2 and "Drifter behavior" in Supplementary Information).

Shipboard CTD niskin-collected samples showed that the unicellular N_2-fixing cyanobacterium, *Crocosphaera watsonii* was abundant relative to historic records and showed a weaker, but similar trend to *Atelocyanobacterium*, with higher abundances in lower salinity, higher phosphate waters along the western portion of Eddy A (Pearson correlation R = 0.71, P=0.05, n=8; Figure 4). Excluding two outlier observations, which we attribute to the patchiness of *Trichodesmium* tufts, *Trichodesmium* and *Crocosphaera* were negatively correlated over this time (Pearson correlation R = -0.94, $P<0.05$, n=10 of 12 samples; Figure 4D) and *Trichodesmium* had similar patchy distributions. Depth profiles of *Atelocyanobacterium nifH* from samples collected from 5 m and 45 m depths

mimicked the patchiness at 25 m, revealing a vertical component to the *Atelocyanobacterium* population, with heterogeneity over the >100 km transit extending to at least 45 m depth (Table 1).

Analyses of historical HOT data revealed a significant negative correlation between phosphate concentrations and salinity for samples collected since 2008 (Pearson correlation $R = -0.86$, $P<0.05$, $n=8$). Moreover, we found a significant positive correlation ($R = 0.87$, $P<0.05$, $n=8$) between *Atelocyanobacterium* abundances and phosphate concentrations during the summer months (Figure 4), but no significant relationship between *Atelocyanobacterium* and salinity was observed for the period 2008-2012.

Bioavailable Fe may also be a limiting nutrient for diazotroph abundances (Sohm et al 2011; Shilova et al., in revision). Although we did not measure Fe concentrations during this cruise, it is plausible that Fe covaried with phosphate, leading to the observed phosphate-to-diazotroph trends. However, Fe is often present in sufficient concentrations at Station ALOHA (Boyle et al 2005), and we recognize that the phosphate-to-iron correlation would have to be quite strong to lead to the observed R values in this study (which is certainly possible since Fe also comes from depth in this region).

Analysis of mesoscale eddies.

Since 1989, 8 of the 10 highest recorded summer phosphate concentrations collected from 25 m depth as part of the HOT monthly sampling program (not including those from BioLINCS) were associated with positive SLA (anticyclonic eddies; Supplementary Figure 4) and just one was in a region of negative SLA. The 10 highest

concentrations of phosphate at Station ALOHA (1989-2012) average 105 ± 17nM (spring) and 116 ± 22nM (summer) (Supplementary Figure 5).

Discussion

Due to their low abundances in the marine environment, and because some cannot be identified precisely by microscopy or by remote sensing, diazotroph distributions are most accurately resolved using targeted molecular approaches. Previous ship-based expeditions have successfully used this approach to quantify diazotrophs over multiple seasons (Church et al., 2009; Langlois et al., 2008; Foster et al., 2009) and large geographic ranges (Moisander et al., 2009; Langlois et al., 2008). These studies demonstrate that nitrogen-fixing communities are patchy and can vary seasonally. Although diazotroph blooms recur every summer (Dore et al., 2008; White et al. 2007), the precise timing and location of blooms is unpredictable. Here we sought to use high-resolution, quasi-Lagrangian sampling to determine 1) whether the patchiness previously reported reflects spatial or temporal variability, and 2) whether abundances can be predicted within the summer and attributed to specific physical and/or chemical factors. Our drifter-based sampling program allowed us to address these objectives by confining the sampling regime to a specific season and depth, and at scales relevant to the ambit of the target organisms (i.e. within ephemeral current fields and during small-scale mixing events; Dickey 2003). This focused approach over a very short period of time surprisingly revealed a wide range of environmental conditions, typically encountered over the course of long-term time-series and ship-based expeditions. Here the *quasi-*

296 Lagrangian nature of the drift allowed us to capture microbial heterogeneity over both
297 space and time, as evidenced by the range of salinities encountered.
298
299 ## Unexpected microbial heterogeneity revealed by high-resolution Lagrangian
300 ## sampling.
301 Over the BioLINCS ESP 10-day time-series, diazotroph concentrations (or *nifH*
302 gene abundances per liter) were among the highest quantified and the most heterogeneous
303 in the region (Fong et al 2008; Church et al 2009), despite quasi-Lagrangian sampling.
304 The variability in diazotroph abundances was similar in magnitude to the variability in
305 abundances seen over monthly time scales during the summer in previous years (Figure
306 3). Further, our results demonstrate that the abundances of N_2-fixing keystone species
307 can display much greater spatio-temporal variability than other groups of microbes,
308 including other members of the cyanobacteria (Table 1). These findings have
309 implications for modeling the distributions of N_2-fixing organisms and rates of nitrogen
310 fixation in open ocean ecosystems. While major population shifts have been documented
311 for several metazoan keystone species (Jackson et al 2001), as a result of the complexity
312 of environmental variation on smaller scales, documenting the same for microbial species
313 has proven difficult unless the species are easily identifiable (such as *Trichodesmium*;
314 Westberry and Siegel, 2006; Davis and McGillicuddy, 2006). Our results indicate that
315 major population fluctuations of keystone microbial species occur on the order of days
316 and kilometers, even when sampling in a quasi-Lagrangian manner (Figures 1, 2).
317
318 ## Evaluation of controls on microbial distributions.

319 The range in salinity encountered during the BioLINCS cruise (0.28) is large for
320 the region, representing 87% of the summer range observed in HOT measurements
321 conducted since 2009 and 28% of the full range for this region since 1989 (Lukas 2001).
322 We observed robust relationships between diazotroph abundances and salinity over the
323 course of the cruise (Supplementary Figure 6), highlighting how small scale fluctuations
324 in ocean physics play critical roles in controlling distributions and abundances of
325 microbes on small scales. Moreover, the extreme heterogeneity observed during our
326 study suggests that high-resolution sampling is key to efficient resolution of the processes
327 the govern diazotroph distributions and abundances within seasons. This population
328 heterogeneity over small scales has important implications for how we assess the
329 metabolic activities of diazotrophs, and how we extrapolate from a limited number of
330 measurements to larger ecosystem-level processes.
331 A combination of ship-based measurements, satellite SLA, FSLE (finite-size
332 Lyapunov exponent) modeling and ocean color indicate that the high heterogeneity in
333 physical and chemical conditions during BioLINCS is the result of both advection and
334 mixing. A calculation of FSLE (e.g. Lehahn et al., 2007) confirms mixing between eddies
335 A and B during the period of sampling. The negative correlation between salinity and
336 phosphate measured during this cruise demonstrates that *Atelocyanobacterium* was
337 abundant within a localized current where salinity and temperature were low, but where
338 phosphate was elevated relative to the surrounding waters. *Atelocyanobacterium*
339 decreased in abundance as the high phosphate current mixed with adjacent waters within
340 the eddy. This trend was also seen with *Crocosphaera* but was not observed for
341 *Trichodesmium* or the "N_2-fixing proteobacteria".

342 Although the relationship between unicellular diazotroph abundances and salinity
343 is not supported in the historic data from Station ALOHA, these microorganisms are
344 positively correlated with phosphate in this region in the summer months since 2008
345 according to HOT datasets (Figure 4). Thus, it appears that lower nutrient concentrations
346 due to stratification can account for low abundances of unicellular diazotrophs during the
347 summer. When combined with eddy-driven nutrient advection into the region year-round
348 and the corresponding enhancement in unicellular diazotrophs, these organisms exhibit
349 patchier distributions in the summer compared to other seasons.
350 Phosphate correlated with *Atelocyanobacterium* abundances more than any other
351 measured parameter in this comprehensive dataset. It must be noted that trace metals and
352 vitamins are not routinely measured during HOT sampling, and it is possible that one of
353 these factors parallels variations in phosphate. Nevertheless, these analyses establish the
354 extent of natural variation and support a link to phosphate for this important diazotroph in
355 the contemporary NPSG. This finding could be used as a basis to predict the fate of
356 *Atelocyanobacterium* in modeled future ocean states.
357

358 ## Local enhancement of unicellular diazotrophs after a mixing event.

359 In the westward transit during BioLINCS (the "inter-eddy transition," Figure 1)
360 there were opposing currents, high but variable nutrients within the mixed layer, and
361 indications of diapycnal mixing. Mixing is apparent at the apex of the ESP drift, where
362 nitrite concentrations are elevated from the nitrite maximum into the shallow photic zone
363 (Figure 2D at 130 – 155 km) and density inversions occur (Supplementary Figure 2C). In
364 this region both *Atelocyanobacterium* and *Crocosphaera* had elevated abundances over

what would be predicted based on the strong physics-driven correlations in Eddy A. Linear correlations between diazotroph abundances and salinity, a conservative property of seawater, indicate that horizontal eddy stirring is the dominant driver of distributions along the northeastward transit. However, in the inter-eddy region the unicellular cyanobacterial diazotrophs (*Atelocyanobacterium* and *Crocosphaera* shown in Supplementary Figure 6) had elevated abundances (25.5-fold and 1.6-fold, respectively) relative to samples with the same salinity in Eddy A. Such observations indicate locally enhanced growth and/or microbial accumulation (Guidi et al., 2012) in the complex inter-eddy region despite a high temperature that is well above the predicted optimal for *Atelocyanobacterium* (Church et al, 2009). In this area *Trichodesmium* had ~13-fold lower abundances than would be expected based on distributions relative to salinity in Eddy A. Unlike the previously strong correlations with environmental factors, the inter-eddy region represents a complex congruence of factors that make diazotroph distributions unpredictable based on horizontal eddy stirring alone.

Anticyclonic eddies linked to surface phosphate concentrations.

Twelve percent of the summer phosphate concentrations sampled since 1989 are below the spring minimum for the region (Supplementary Figure 5), presumably reflecting increased stratification during the summer months and lower vertical nutrient supply. Satellite altimetry and HOT measurements were used to determine whether the passage of mesoscale eddies through the ALOHA sampling region is a major source of biogeochemical variability in that time-series. Indeed, the highest concentrations of recorded phosphate in the summer months were within mesoscale *anticyclonic* eddies,

388 (Supplementary Figures 4, 5B), which was unexpected. High stratification and lower
389 background nutrient concentrations in surface waters during the summer amplify the
390 importance of small nutrient increases in the upper ocean, suggesting that the highest
391 phosphate samples in summer are the result of increased phosphate input rather than
392 lower biological draw-down. Mesoscale eddies impart significant variability to ocean
393 biogeochemistry at Station ALOHA (Church et al., 2009) and the impacts of such events
394 appear most pronounced during the summer, resulting in a larger range of phosphate
395 concentrations in the photic zone over the summer months than other seasons This
396 extreme range of conditions has important implications for the growth and activities of
397 microorganisms.

398 An excess of phosphate in the photic zone can be caused by: 1) recent delivery
399 from depth, 2) accumulation due to low demand from the microbial community (i.e.
400 phosphate is not a limiting nutrient) or 3) a localized biological or atmospheric source of
401 phosphate. While we did not measure phosphate flux during the BioLINCS cruise, the
402 strong salinity-phosphate relationship suggests a recent delivery of low salinity, high
403 phosphate water from depth into the region of sampling. This hypothesis is supported by
404 the frequency of samples measured by the HOT series with below-average salinity and
405 above-average phosphate (Supplementary Figure 5B). 11 of the 14 high-phosphate
406 samples collected during summers from 25 m depth have salinities below the average for
407 the HOT summer salinity dataset. We believe these highest-phosphate concentrations are
408 derived from recent vertical inputs.

409 A phosphate-stimulated increase in nitrogen fixation activity would lead to a
410 negative correlation between phosphate concentration and diazotroph abundance, as

411 microbes deplete phosphate from nitrogen-limited seawater at steady-state (i.e. no
412 external phosphate input). During BioLINCS, we observed the stirring of near-record
413 high-phosphate seawater with very low-phosphate seawater. The positive correlation
414 between the abundances of unicellular diazotrophs and phosphate likely reflects the
415 mixing of waters where these organisms are nutrient-limited (low abundance) vs. those
416 where they are nutrient-replete (high abundance). The positive correlation in historic
417 HOT records, which reflect a variety of ocean states, was unexpected. While the link
418 with phosphate (and not salinity) is clear, we cannot yet fully explain the mechanism that
419 leads to this correlation.
420

421 ## Implications.

422 Marine microorganisms can display high heterogeneity over time and space, and
423 variations in diazotroph community composition are often associated with significant
424 changes in nitrogen fixation rates (Church et al 2009; Shiozaki et al 2013; Wilson et al
425 2013). Understanding the controls on distributions of microbial populations is crucial for
426 predicting future changes in ocean biogeochemistry (Giovannoni and Vergin 2012; Zehr
427 et al 2011). The BioLINCS cruise demonstrates the promise of next-generation
428 autonomous *in situ* sensors for revealing such processes. Mesoscale physical features
429 including open-ocean eddies create ephemeral habitats with small-scale physical and
430 chemical heterogeneity that has major consequences for microbial distributions and
431 metabolic activities. This study shows that N_2-fixing cyanobacterial abundances in
432 summer are highly variable relative to other important groups of microbes and are

433 inextricably coupled to small-scale variations in nutrients caused by transport and mixing
434 of water masses in the Station ALOHA region.

435 The projected increases in mesoscale activity in the region (Murakami et al 2013)
436 should result in higher microbial patchiness at Station ALOHA, further complicating
437 interpretations of station-based biogeochemical time-series data. A single short-term,
438 high-resolution time-series in this targeted region encountered a range of conditions
439 comparable to years of summer sampling at Station ALOHA and showed that microbial
440 distributions were clearly correlated with environmental factors. Monthly time series
441 programs that randomly sample open ocean eddies show the same correlations over
442 sustained, long-term sampling. Long-term changes in phosphate have been documented
443 at Station ALOHA (Karl et al 2001), and recent studies have described a reversal of the
444 long-term phosphate depletion in the region (Karl et al 2014). We sampled on the cusp
445 of this reversal in 2011 and our observations may reflect a corresponding regime change,
446 which we would predict to be coupled with an increase in unicellular diazotrophs. Based
447 on the current study, it appears that these types of nutrient changes directly affect
448 diazotroph community composition that result in spatiotemporal changes in nitrogen
449 fixation. Given these characteristics along with their keystone species status, the
450 importance of their biogeochemical function and the regularity with which they are
451 quantified in the open ocean (Church et al 2005; Fong et al 2008; Church et al 2009;
452 Church et al 2008; Moisander et al 2010), diazotroph populations can effectively serve as
453 sentinel species for detecting ecosystem change.
454

455 **Acknowledgments**

This work was funded by the MEGAMER facility grant by the Gordon and Betty Moore Foundation to JPZ, the David and Lucille Packard Foundation to CAS (through grants allocated to MBARI), the NSF Center for Microbial Oceanography, Research and Education (C-MORE grant # EF04-24599) to JPZ and DMK, the Gordon and Betty Moore Foundation Marine Microbiology Investigator Program (JPZ and DMK), NSF grants OCE0425363 to JPZ and MJC, OCE0850827 to MJC (for historical *nifH* abundance measurements from Station ALOHA) and OCE0926766 to MJC and DMK (for support of the HOT program). Many thanks to Chris Edwards, Mariona Segura i Noguera, Ken Doggett, Susan Curless, Karin Björkman, Tara Clemente, Sara Thomas, Gene Massion, Kendra Turk, Ariel Rabines, Chris Preston, Nilo Alvarado, Brent Roman, Blake Watkins and we are grateful for the expertise of the crew of the R/V *Kilo Moana*.

Supplementary Information is available at The ISME Journal's website.

The authors declare no conflict of interest.

References

1. Ascani F, Richards KJ, Firing E, Grant S, Johnson KS, Jia Y *et al*. (2013). Physical and biological controls of nitrate concentrations in the upper subtropical North Pacific Ocean. *Deep-Sea Res II* **93**: 119-134.

2. Boyle EA, Bergquist BA, Kayser RA, Mahowald N (2005). Iron, manganese, and lead at Hawaii Ocean Time-series station ALOHA: Temporal variability and an intermediate water hydrothermal plume. *Geochim Cosmochim Acta* **69:** 933-952.

3. Carpenter EJ, Capone, DG (2008). Nitrogen fixation in the marine environment. *Nitrogen in the Marine Environment*, 2 edn. Academic Press: Burlington, MA. pp 141-198.

4. Church MJ, Short CM, Jenkins BD, Karl DM, Zehr JP (2005). Temporal patterns of nitrogenase gene (nifH) expression in the oligotrophic North Pacific Ocean. *Appl Environ Microb* **71:** 5362-5370.

5. Church MJ, Björkman KM, Karl DM, Saito MA, Zehr JP (2008). Regional distributions of nitrogen-fixing bacteria in the Pacific Ocean. *Limnol Oceanogr* **53:** 63-77.

6. Church MJ, Mahaffey C, Letelier RM, Lukas R, Zehr JP, Karl DM (2009). Physical forcing of nitrogen fixation and diazotroph community structure in the North Pacific subtropical gyre. *Global Biogeochem Cy* **23**.

7. Davis, CS, McGillicuddy DJ (2006). Transatlantic abundance of the N(2)-fixing colonial cyanobacterium *Trichodesmium*. *Science* **312**, 1517.

8. Dickey TD (2003). Emerging ocean observations for interdisciplinary data assimilation systems. *J Mar Sys* **40-41:** 5-48.

9. Dore JE, Karl DM (1996). Nitrification in the euphotic zone as a source for nitrite, nitrate, and nitrous oxide at Station ALOHA. *Limnol Oceanogr* **41:** 1619-1628.

10. Dore JE, Letelier RM, Church MJ, Lukas R, Karl DM (2008). Summer phytoplankton blooms in the oligotrophic North Pacific Subtropical Gyre: Historical perspectives and recent observations. *Prog Oceanogr* **76**: 2-38.

11. Dyhrman ST, Chappell PD, Haley ST, Moffett JW, Orchard ED, *et al*. (2006). Phosphonate utilization by the globally important marine diazotroph Trichodesmium. *Nature* **439**, 68.

12. Fong AA, Karl DM, Lukas R, Letelier RM, Zehr JP, Church MJ (2008). Nitrogen fixation in an anticyclonic eddy in the oligotrophic North Pacific Ocean. *Isme J* **2:** 663-676.

13. Foster RA, Paytan A, Zehr J (2009). Seasonality of N_2 fixation and *nifH* gene diversity in the Gulf of Aquaba (Red Sea). *Limnol Oceanogr* **54:** 219-233.

14. Giovannoni SJ, Vergin KL (2012). Seasonality in ocean microbial communities. *Science* **335:** 671-676.

15. Guidi L, Calil PHR, Duhamel S, Björkman KM, Doney SC *et al.* (2012). Does eddy-eddy interaction control surface phytoplankton distribution and carbon export in the North Pacific Subtropical Gyre? *J Geophys Res* **117**: 1-12.

16. Hashihama F, Furuya K, Kitajima S, Takeda S, Tekemura T *et al.* (2009). Macro-scale exhaustion of surface phosphate by dinitrogen fixation in the western North Pacific. *Geophys Res Lett* **36**.

17. Ilikchyan IN, McKay RML, Kutovaya OA, Condon R, Bullerjahn GS (2010). Seasonal expression of the picocyanobacterial phosphonate transporter gene phnD in the Sargasso Sea. Front Microbiol doi: 10.3389/fmicb.2010.00135

18. Jackson JBC, Kirby MX, Berger WH, Bjorndal KA, Botsford LW, Bourque BJ *et al* (2001). Historical overfishing and the recent collapse of coastal ecosystems. *Science* **293:** 629-638.

19. Johnson KS, Riser SC, Karl DM (2010). Nitrate supply from deep to near-surface waters of the North Pacific subtropical gyre. *Nature* **465:** 1062-1065.

20. Karl DM, Tien G (1992). MAGIC - a Sensitive and Precise Method for Measuring Dissolved Phosphorus in Aquatic Environments. *Limnol Oceanogr* **37:** 105-116.

21. Karl DM, Bjorkman KM, Dore JE, Fujieki L, Hebel DV, Houlihan T *et al* (2001). Ecological nitrogen-to-phosphorus stoichiometry at station ALOHA. *Deep-Sea Res Pt II* **48:** 1529-1566.

22. Karl DM, Church MJ, Dore JE, Letelier RM, Mahaffey C (2012). Predictable and efficient carbon sequestration in the North Pacific Ocean supported by symbiotic nitrogen fixation. *Proc Natl Acad Sci USA* **109:** 1842-1849.

23. Karl DM (2014). Microbially-mediated transformations of phosphorus in the sea: New views of an old cycle. *Ann Rev Mar Sci* **6**, *in press.*

24. Langlois RJ, Hummer D, LaRoche J (2008). Abundances and distributions of the dominant nifH phylotypes in the Northern Atlantic Ocean. *Appl Environ Microb* **74**: 1922-1931, doi:10.1128/AEM.01720-07.

25. Lehahn Y, d'Ovidio F, Lévy M, Heiftez E (2007). Stirring of the northeast Atlantic spring bloom: A Lagrangian analysis based on multisatellite data. *J. Geophys Res* **112**, C08005.

26. Lukas R (2001). Freshening of the upper thermocline in the North Pacific subtropical gyre associated with decadal changes of rainfall. *Geophys Res Lett* **28:** 3485-3488.

27. Moisander PH, Beinart RA, Hewson I, White AE, Johnson KS, Carlson CA *et al* (2010). Unicellular cyanobacterial distributions broaden the oceanic N2 fixation domain. *Science* **327:** 1512-1514.

28. Murakami H, Wang, B., Li, T. Kitoh, A. (2013). Projected increase in tropical cyclones near Hawaii. *Nature Climate Change,* doi:10.1038/nclimate1890.

29. Nolan KM (2008). Characteristics and water properties of mesoscale eddies in the region of Station ALOHA. *University of Hawaii, Department of Oceanography Masters Thesis*.

30. Ottesen EA, C.R. Young, J.M. Eppley, J.P. Ryan, F.P. Chavez, C.A. Scholin, E.F. DeLong (2013). Pattern and synchrony of gene expression among sympatric marine microbial populations. *Proc Natl Acad Sci U S A* **110:** E488-E497.

31. Preston CM, Marin R, Jensen SD, Feldman J, Birch JM, Massion EI *et al* (2009). Near real-time, autonomous detection of marine bacterioplankton on a coastal mooring in Monterey Bay, California, using rRNA-targeted DNA probes. *Environ Microbiol* **11:** 1168-1180.

32. Preston CM, Harris A, Ryan JP, Roman B, Marin R, Jensen S *et al* (2011). Underwater application of quantitative PCR on an ocean mooring. *Plos One* **6**.

33. Robidart JC, Preston CM, Paerl RW, Turk KA, Mosier AC, Francis CA *et al* (2012). Seasonal *Synechococcus* and *Thaumarchaeal* population dynamics examined with high resolution with remote *in situ* instrumentation. *ISME J* **6:** 513-523.

34. Scholin CA (2013). Ecogenomic sensors. In: Levin SA (ed.) Encyclopedia of Biodiversity, second edition, Volume 2: 690-700. Waltham, MA: Academic Press.

35. Shilova IN, Robidart JC, Tripp HJ, Turk-Kubo K, Wawrick B, Thompson A *et al* (2014). Development and application of a microarray for assessing gene transcription in open ocean microbial communities. *ISME J*, in revision.

36. Shiozaki T, T. Kodama, S. Kitajima, M. Sato, K. Furuya (2013). Advective transport of diazotrophs and importance of their nitrogen fixation on new primary production in the western Pacific warm pool. *Limnol Oceanogr* **58:** 49-60.

609 37. Sohm JA, Webb EA, Capone DG (2011). Emerging patterns of marine nitrogen
610 fixation. *Nat Rev Microbiol* **9:** 499-508.
611
612 38. Thompson AW, Foster RA, Krupke A, Carter BJ, Musat N, Vaulot D *et al* (2012).
613 Unicellular cyanobacterium symbiotic with a single-celled Eukaryotic alga. *Science*
614 **337:** 1546-1550.
615
616 39. Westberry TK, Siegel DA (2006). Spatial and temporal distribution of
617 *Trichodesmium* blooms in the world's oceans. *Global Biogeochem Cycles* **20** (4):
618 GB4016, doi:10.1029/2005GB002673.
619
620 40. White AE, Spitz YH, Letelier RM (2007). What factors are driving summer
621 phytoplankton blooms in the North Pacific Subtropical Gyre? *J Geophys Res* **112**:
622 C12006, doi:10.1029/2007JC004129
623
624 41. White AE, Karl DM, Björkman KM, Beversdorf LJ, Letelier RM (2010). Production
625 of organic matter by *Trichodesmium* IMS101 as a function of phosphorus source.
626 *Limnol Oceanogr* **55**, 1755.
627
628 42. Wilson S, D. del Valle, J. Robidart, J. Zehr, D. Karl (2013). Dissolved hydrogen and
629 nitrogen fixation in the oligotrophic North Pacific Subtropical Gyre. *Environ*
630 *Microbiol Reports* **5** (5): 697-704.
631
632 43. Zehr JP, Robidart J, Scholin C (2011). Marine microbes, biogeochemical cycles,
633 and global climate change. *Microbe* **6**: 169-175.
634
635
636
637

638

639 **Figure Captions**

640

641 Figure 1. BioLINCS environmental setting. (**A**) Sea level anomaly (SLA: contours
642 overlaid on all panels), sea surface temperature (SST) and near-surface chlorophyll
643 concentrations are averages of satellite data for 6-20 September 2011. The grey/black
644 track shows the drift path of the instrumented platform (ESP, CTD and ADCP), which
645 began at the southernmost point. SLA image depicts Eddies A and B, which influenced
646 the ESP drift trajectory and are described in the text. The clockwise circulation of Eddy
647 A, and associated stirring of regional water types, is evident in the SST and chlorophyll
648 patterns. Station ALOHA is marked by the circle+ symbol. (**B**) GOES SST from 12-13
649 September 2011 (nighttime). (**C**) Salinity along the ESP drift track, upper 80 m. (**D**) ESP
650 drifter float (left) and base (right) are connected via an electro-mechanical cable. The
651 ESP is sealed within the grey cylindrical pressure housing mounted to the platform base.

652

653 Figure 2. ESP drift contours of nutrient concentrations and ecological observations. (**A**)
654 Platform velocity (speed in color, direction in track). Earth-referenced velocity of the
655 ESP was determined from the time-series of its GPS position. (**B**) Platform quasi-
656 Lagrangian behavior based on the ESP-relative speed of water 3 m above the ESP. A
657 water velocity of zero indicates Lagrangian movement (*i.e.* perfect movement with the
658 currents). (**C**) Salinity, with abundances of *Atelocyanobacterium* (in *nifH* gene copies per
659 L). (D) *Atelocyanobacterium* are in red, *Trichodesmium* in orange and *Crocosphaera* in
660 blue, plotted relative to the cruise transit distance. Solid lines indicate ESP-collected data
661 and dotted lines are data from seawater collected from CTD niskins on board the ship.

662 Diazotroph abundances are in agreement between the ESP and CTD. Chlorophyll,
663 phosphate, nitrite and density are plotted vs. depth and transit distance for this same
664 period. Phosphate concentrations in surface waters are high but variable during the
665 cruise. Relatively high nitrite concentrations extend from depth to the surface waters in
666 the eastern portion of the inter-eddy transition zone, as the ESP circled twice due to
667 contrasting currents. Numbers in red indicate ESP sample numbers (samples taken 16
668 hours apart), corresponding with locations in Supplementary Figure 1. Stars indicate
669 regions of lowest SLA sampled, where nutrients are highest in the surface waters. The
670 red star in panels A and D also corresponds with the apex of the ESP transit.
671
672 Figure 3. Time series for the three most abundant diazotrophs during the present study
673 and historical observations from Station ALOHA. (**A**) *Atelocyanobacterium*,
674 *Trichodesmium* and *Crocosphaera* abundances over three years of monthly sampling at
675 Station ALOHA (2008-2011). Summer months are darkened in grey. (**B**) Abundances of
676 the same organisms during BioLINCS. See Supplementary Figure 3 for physical
677 orientation by ESP sample number. Dotted lines delineate the range of abundances
678 quantified during BioLINCS, demonstrating a heterogeneity in the *Atelocyanobacterium*
679 and *Trichodesmium* populations that is comparable to the three years of summer
680 abundance data from ALOHA.
681
682 Figure 4: Linear regressions with phosphate sampled by ESP and ship-based sampling.
683 (**A**) The clear relationship between salinity and phosphate during the BioLINCS cruise
684 allowed extrapolation of phosphate concentrations using salinity data, from ESP-

685 collected samples. (**B**) Log of *Atelocyanobacterium* abundances vs. phosphate
686 concentration. For remaining panels, squares correspond to BioLINCS Eddy A samples,
687 bold squares correspond with BioLINCS inter-eddy transition zone samples, and dashed
688 squares correspond with HOT data since 2008. There is a clear relationship between
689 *Atelocyanobacterium* abundances and phosphate concentration in the summer for all
690 datasets since 2008 (note that here we show R^2 values, whereas Pearson correlation R
691 values are reported in the main text). (**C**) Positive relationship between the log of
692 *Crocosphaera* abundances and phosphate concentrations ($P = 0.05$). (**D**) Negative
693 relationship between the log of *Trichodesmium* abundance vs. phosphate concentration ($P
694 > 0.05$). Inset shows the same log of *Trichodesmium* abundances vs. *Crocosphaera*
695 abundances ($R = -0.88$; $P < 0.05$); Red "X" designate the two outliers of this correlation.
696 Abundances in the inter-eddy transition zone are elevated for the unicellular
697 cyanobacteria, and depleted for *Trichodesmium*.
698
699 Table 1. Microbial population patchiness. Patchiness measured by ESP (15 sandwich
700 hybridization array samples and 14 qPCR samples) and from ship-collected CTD niskin
701 samples (flow cytometric (FCM) and qPCR samples, 9 each) at 25 m depth unless stated
702 otherwise. "N/A" signifies that no data were collected for these parameters. For qPCR
703 abundances, ">" means that the lower gene counts were below the limit of quantification
704 (5 copies) for these targets. Variation in diazotroph populations well exceeds variation in
705 other cyanobacteria populations as well as picoeukaryotes and "heterotrophs."
706 Heterotrophs are defined as SAR11, SAR86 and marine Roseobacter clades for

hybridization array (probes described in Preston *et al.,* 2009), and as all non-fluorescing microbes for flow cytometry counts.

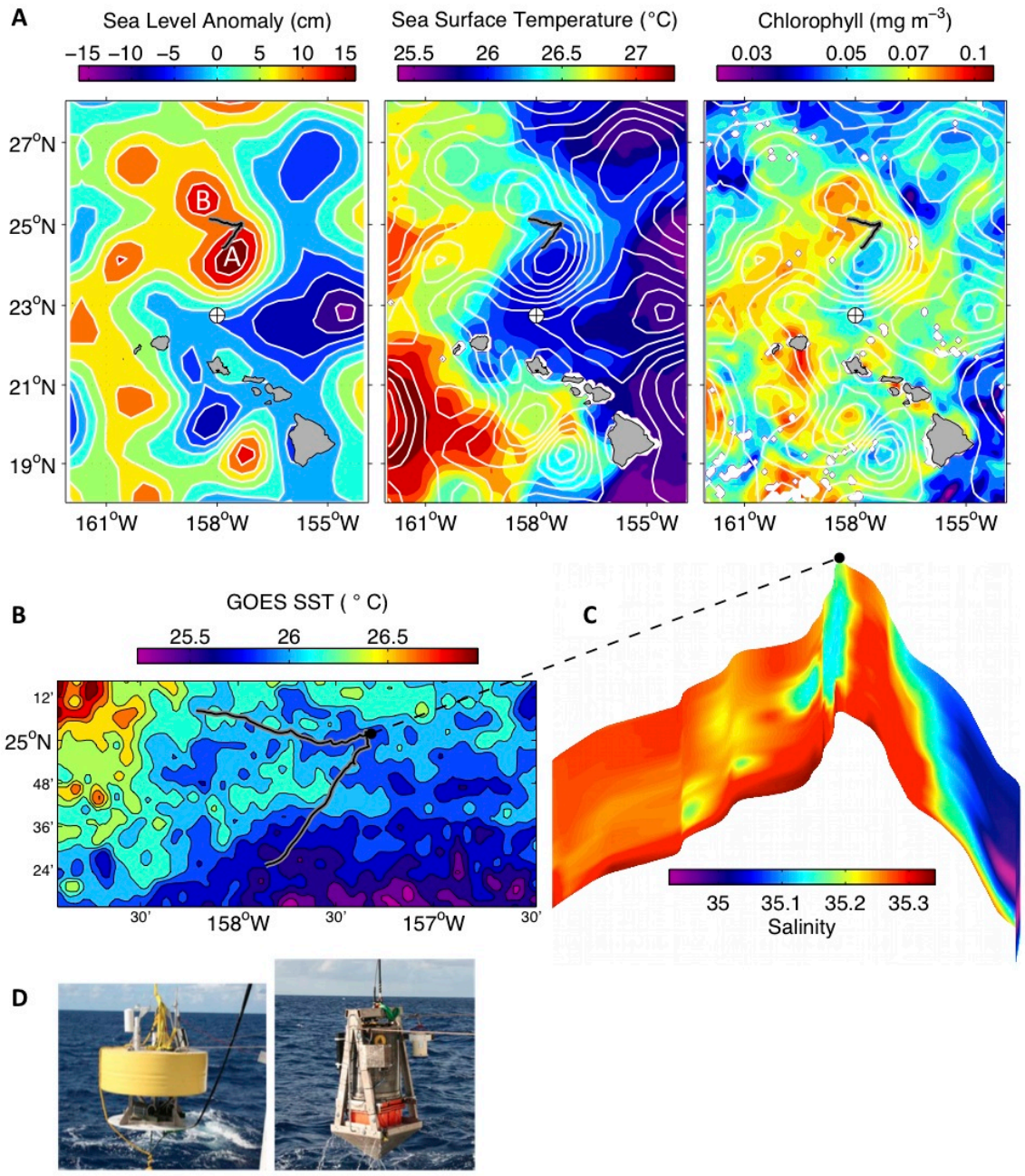
A
Sea Level Anomaly (cm)
−15 −10 −5 0 5 10 15
Sea Surface Temperature (°C)
25.5 26 26.5 27
Chlorophyll (mg m−3)
0.03 0.05 0.07 0.1
27°N
25°N
23°N
21°N
19°N
B
A
161°W 158°W 155°W
B
GOES SST (° C)
25.5 26 26.5
12'
25°N
48'
36'
24'
30' 158°W 30' 157°W 30'
C
35 35.1 35.2 35.3
Salinity
D

710

711

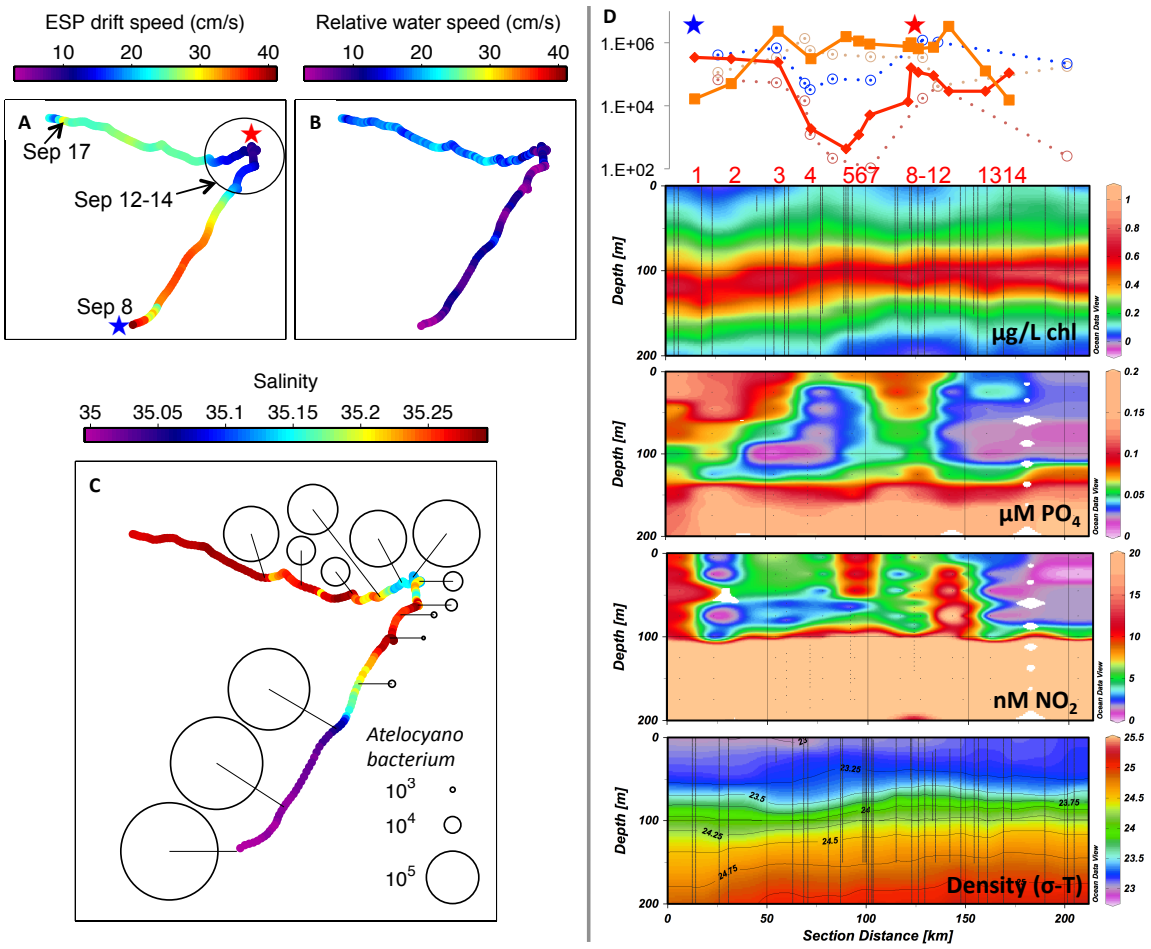
ESP drift speed (cm/s)
10 20 30 40
Relative water speed (cm/s)
10 20 30 40
A
Sep 17
Sep 12-14
Sep 8
B
Salinity
35 35.05 35.1 35.15 35.2 35.25
C
Atelocyano bacterium
10^3
10^4
10^5
D
1.E+06
1.E+04
1.E+02
1 2 3 4 567 8-12 1314
Depth [m]
µg/L chl
µM PO4
nM NO2
Density (σ-T)
Section Distance [km]

712

713

714

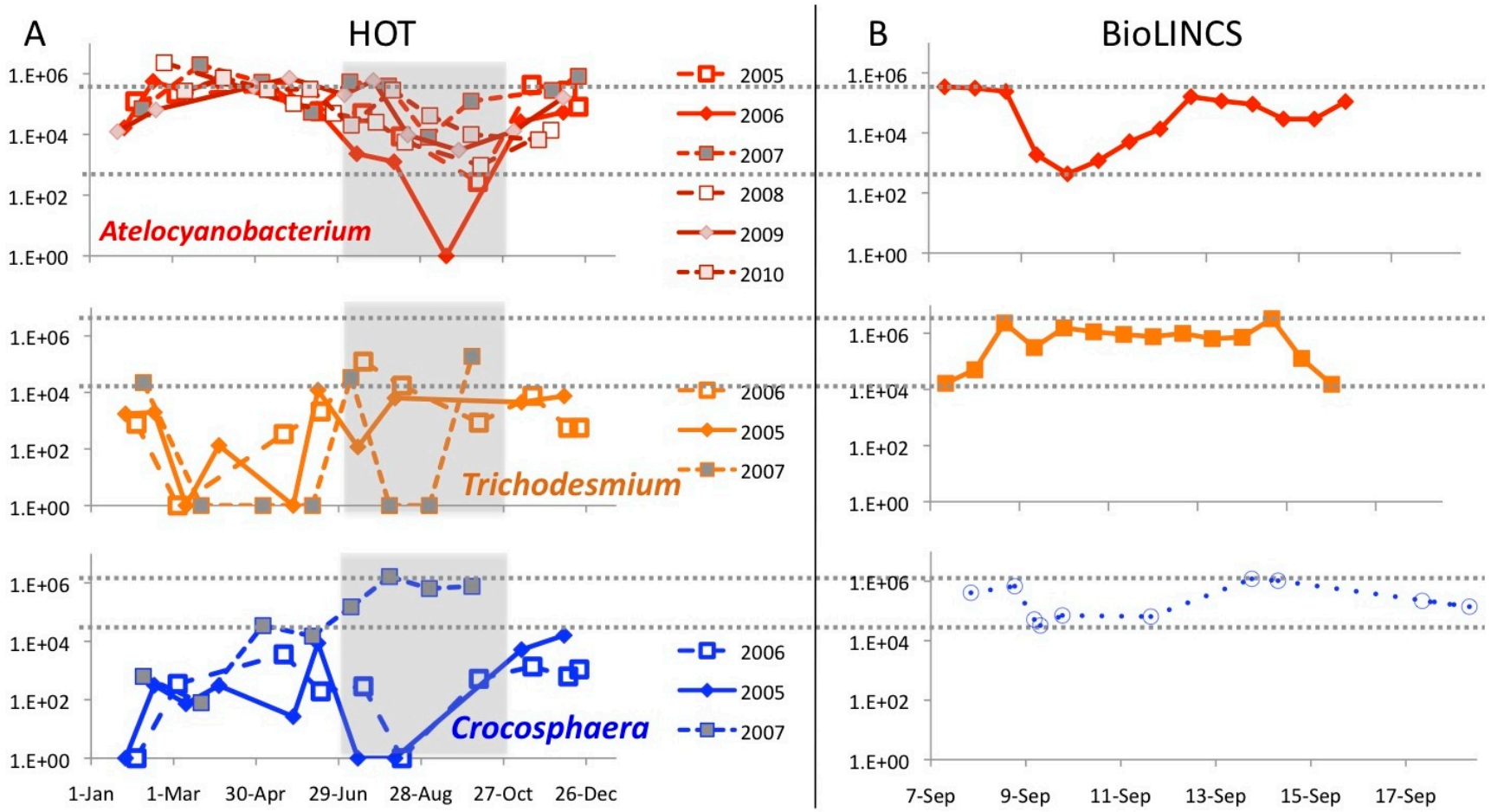
A
HOT
B
BioLINCS
1.E+06
1.E+04
1.E+02
1.E+00
Atelocyanobacterium
2005
2006
2007
2008
2009
2010
Trichodesmium
2006
2005
2007
Crocosphaera
2006
2005
2007
1-Jan
1-Mar
30-Apr
29-Jun
28-Aug
27-Oct
26-Dec
7-Sep
9-Sep
11-Sep
13-Sep
15-Sep
17-Sep

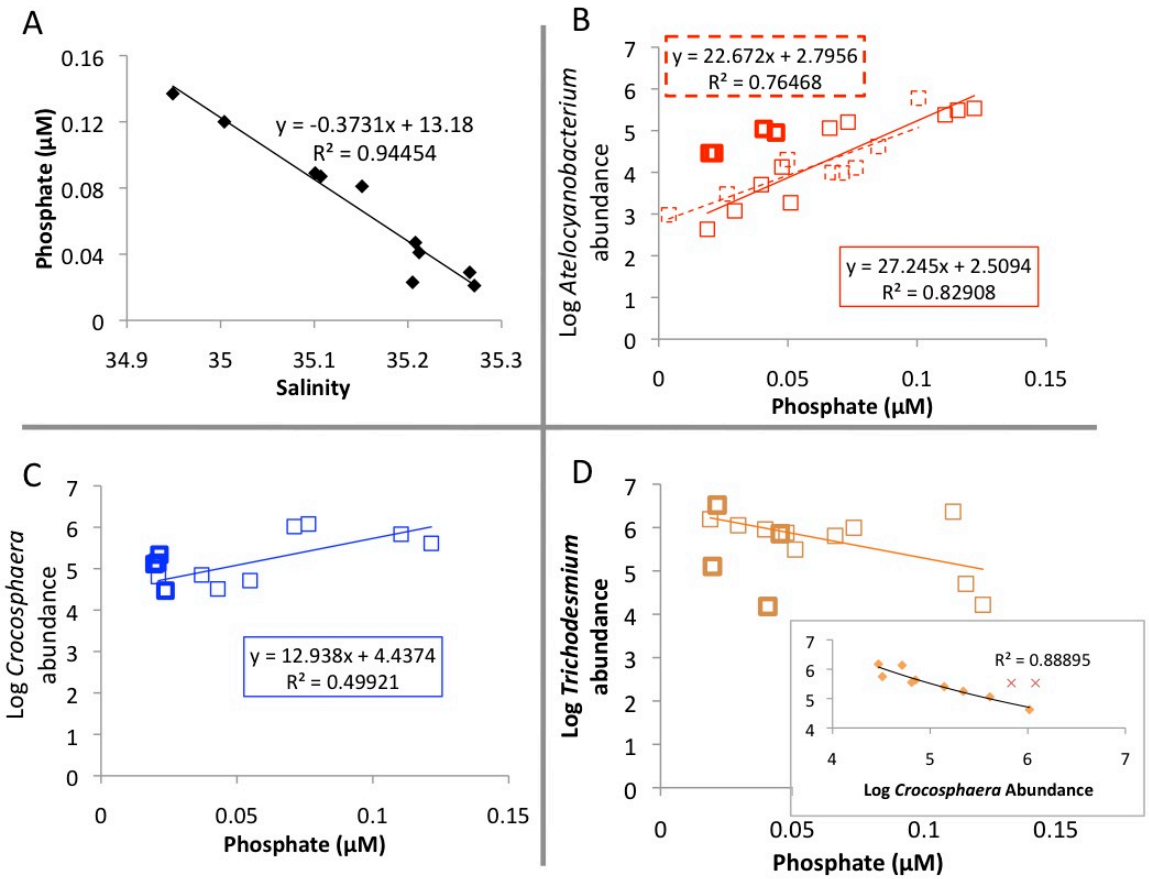
A
Phosphate (µM)
0.16
0.12
0.08
0.04
0
y = -0.3731x + 13.18
R² = 0.94454
34.9
35
35.1
35.2
35.3
Salinity
B
Log Atelocyanobacterium abundance
y = 22.672x + 2.7956
R² = 0.76468
y = 27.245x + 2.5094
R² = 0.82908
0
0.05
0.1
0.15
Phosphate (µM)
C
Log Crocosphaera abundance
y = 12.938x + 4.4374
R² = 0.49921
Phosphate (µM)
D
Log Trichodesmium abundance
R² = 0.88895
Log Crocosphaera Abundance
Phosphate (µM)

716

717

Ratio Most:Least Abundant		
	ESP	Ship
	Array (n=15)	FCM (n=9)
Prochlorococcus	2.53	1.31
Synechococcus		1.92
Picoeukaryotes	N/A	1.74
Heterotrophs*	2.15	1.10
	qPCR (n=14)	qPCR (n=16)
5 meter depth *Atelocyanobacterium*	N/A	176.86
25 meter depth *Atelocyanobacterium*	792.59	627.56
45 meter depth *Atelocyanobacterium*	N/A	1636.43
75 meter depth *Atelocyanobacterium*	N/A	48.45
Trichodesmium	217.75	32.38
Crocosphaera	N/A	37.04
Gamma proteobacteria	>19.32	>8.93
Richelia-Rhizosolenia symb.	N/A	>13.22
Richelia-Hemialus symb.	N/A	>8.57
Synechococcus II, cluster 1	N/A	20.14
Synechococcus II, cluster 2	N/A	2.5
Synechococcus III	N/A	6.6

718